DIRECT NUMERICAL SIMULATION OF PARTICLES DISPERSION IN SUPERSONIC SHEAR LAYERS

Jean-Luc Estivalezes Yannick Bury
ONERA DMAE
2 Av Edouard Belin BP 4025
31055 TOULOUSE FRANCE

ABSTRACT

Particles dispersion plays an important role in many industrial applications such as combustion, pollution control and also in experimental measurements like Laser Doppler Velocimetry. In this last case, particles are supposed to have the same behaviour as fluid particles in order to give relevance to the experimental measure. However it has be shown Jacquin et al. (1991) that noticeable errors can appear in the rms velocity measurement of supersonic jet or shear layer, even if care has been taken concerning particle seeding of the flow. The aim of this paper is to use direct numerical simulation of particle-gaz flow to investigate this phenomenon.

INTRODUCTION

We are mainly concerned with three dimensional supersonic mixing layers. In such flows, beyond convective Mach number greater than 0.6, stability theory and direct numerical simulations show that oblique modes are much more rapidly amplified than two dimensional modes Sandham and Reynolds (1991) (which correspond to the incompressible modes) leading to Λ vortices which are staggered in the streamwise direction. This particular behaviour could involve strong modification in mixing process. The object of the present work is to investigate how those highly three dimensional structures influence particles dispersion.

NUMERICAL METHOD

Governing equations

The full time dependent Navier-Stokes equations for three-dimensional fluid motion are written in a non-dimensional conservative form. For a three-dimensional cylindrical case, we have :

$$\frac{\partial U}{\partial t}+\frac{\partial F}{\partial x}+\frac{\partial G}{\partial y}+\frac{\partial H}{\partial z}-\frac{\partial F_v}{\partial x}-\frac{\partial G_v}{\partial y}-\frac{\partial H_v}{\partial z}=0 \quad (1)$$

U is the vector of conservative variables :

$$U=(\rho,\ \rho u,\ \rho v,\ \rho w,\ E)^T \quad (2)$$

F, G, H are the non-viscous fluxes. F_v, G_v, H_v are the viscous contributions.

Here ρ, u, v, w, E denote respectively the density, fluid velocity components in the directions x, y and z, and the total energy (sum of the internal and kinetic energy). Non-dimensionalization of these equations is with respect to reference quantities, namely a reference length L^*, velocity U_1^*, density ρ_1^*, temperature T_1^*, and viscosity μ_1^*. L^*/U_1^* is the time reference scale, while $\rho_1^* U_1^{*2}$ is the pressure (and total energy) reference. The superscript * refers to a dimensional quantity. In our case, as we are interested by a temporal mixing layer, the reference lenght is chosen as the initial vorticity thickness of the longitudinal velocity profile : $L=\delta_{\omega 0}$, the reference velocity, temperature, density and viscoity are respectively U_1^*, T_1^*, ρ_1^*, μ_1^*, which are the far field values of the upper stream (cf 1). Using this non-dimensional scheme, we introduce the Reynolds number of the flow $Re=\rho_1^* U_1^* \delta_{\omega 0}/\mu_1^*$ and the Mach number which is in our case equal to the convective Mach number M_c is $M=U_1^*/\sqrt{\gamma \mathcal{R}^* T_1^*}$, where $\mathcal{R}^*=287.15\ J\ kg^{-1}\ K^{-1}$. The Prandtl number, assumed to be constant, is defined by

$Pr = \mu^* C_p^* / k^*$ where k^* is the thermal conductivity. The viscosity follows Sutherland's law. The system is completed by the definition of the total energy, written in non-dimensional form as :

$$E = \frac{p}{\gamma - 1} + \frac{1}{2}\rho(u^2 + v^2 + w^2) \tag{3}$$

and by the perfect gas law :

$$\frac{p}{\rho} = \frac{T}{\gamma M^2} \tag{4}$$

Numerical scheme

Equations are solved using a finite volume high order extension of MacCormack's scheme due to Gottlieb and Turkel Gottlieb and Turkel (1976). This scheme has already been used by many authors for boundary layer simulations Bayliss, A. et al (1985), Ducros, F. (1995), for mixing layer simulations Ragab and Sheen (1991), Ragab and Sheen (1992), Tang, W. et al (1989), and for supersonic jet flow studies Mankbadi et al (1994). Based on predictor corrector phases, the scheme is explicit, second order accurate in time and fourth order in space. The time step Δt follows a CFL condition, and Fourier criteria. Extension to three dimensions and to the complete fluid motion equations is done through a directional splitting sequence :

$$\begin{aligned} U^{n+2} &= L_{zv}^- L_{yv}^- L_{xv}^- L_z^- L_y^- L_x^- L_{zv}^+ L_{yv}^+ L_{xv}^+ L_z^+ L_y^+ L_x^+ U^n \\ U^{n+4} &= L_{xv}^+ L_{yv}^+ L_{zv}^+ L_x^+ L_y^+ L_z^+ L_{xv}^- L_{yv}^- L_{zv}^- L_x^- L_y^- L_z^- U^{n+2} \end{aligned} \tag{5}$$

L_x, L_y, L_z, L_{xv}, L_{yv} and L_{zv} correspond respectively to the implementation of F, G, H, F_v, G_v and H_v. L_i^+ (with $i = x$, y, or z) refers to a sweep in the direction i with forward predictor and backward corrector. The alternate version L_i^-, employs a backward predictor and forward corrector.

Boundary conditions and initial conditions

Because we deal with temporal mixing layer, periodic boundary conditions are used in the streamwise and spanwise directions (x and y directions). As we are considering an unbounded compressible mixing layer, non reflective boundary conditions based on Thompson Thompson (1987), Gamet and Estivalezes (1995) idea are used in the cross-stream direction (z direction).

Initialization of velocity, temperature and density fields consists of two parts, the mean profiles and the pertubations from linear stability theory Sandham and Reynolds (1991).

The mean non dimensional velocity profile in the streamwise direction is :

$$\overline{u} = \tanh(2z) \tag{6}$$

The mean non dimensional temperature and density profiles are given by Crocco relations:

$$\begin{aligned} \overline{T} &= M_c^2 \frac{(\gamma - 1)}{2}(1 - \overline{u}^2) + 1 \\ \overline{\rho} &= \frac{1}{\overline{T}} \end{aligned} \tag{7}$$

The initial disturbance field is specified by :

$$\begin{aligned} u' = {} & A_1 \mathrm{Real}\{\hat{u}(\alpha, 0) e^{i(\alpha x + \phi)}\} + \\ & A_2 \mathrm{Real}\{\hat{u}(\alpha, \beta) e^{i(\alpha x + \beta y)} + \hat{u}(\alpha, -\beta) e^{i(\alpha x - \beta y)}\} \end{aligned} \tag{8}$$

where $\hat{u}(\alpha, \beta)$ is an eigenfunction of the linear instability wave with streamwise wavelenght $L_x = 2\pi/\alpha = 13.36\,\delta_{\omega 0}$ and spanwise wavelenght $L_y = 2\pi/\beta = 13.36\,\delta_{\omega 0}$. It consists of a two dimensional and a pair of oblique waves. The angle of the oblique waves with the x direction is 45^o degree. Similar disturbances are added for ρ', v', w', and T'. Here the value of the phase is $\pi/2$ in order to get the translative mode Sandham and Reynolds (1991), Pierrhumbert and Widnall (1982).

Particles dispersion simulation

The following assumptions are made for the dispersed phase :

- dilute flow,
- all particles are rigid spheres,
- particle-particle interactions are neglected,
- density of particles is much larger than that of the fluid
- gravity is negligible.

With those assumptions the non dimensional particles motion equation writes :

$$\begin{aligned} \frac{d\vec{V}}{dt} &= \frac{C_d}{St}(\vec{U} - \vec{V}) \\ \frac{d\vec{X}}{dt} &= \vec{V} \end{aligned} \tag{9}$$

where $\vec{U}$ is the fluid velocity at the particle location and $\vec{V}$ is the particle velocity.

$St = \frac{\rho_p d_p^2}{18\mu} \frac{U_1^*}{\delta_{\omega_0}}$ is the Stokes number and C_d is the modified Stokes drag factor coefficient ($C_d = 1 + 0.15 Re_p^{0.687}$, for particle Reynolds number $Re_p = |\vec{U} - \vec{V}| d_p/\nu$ less than 1000).

The velocity and particle position equations are integrated by fourth order Runge and Kutta methods. Fluid velocity at particles positions is interpolated by fourth order Hermite polynomia interpolations.

RESULS FOR PARTICLE DISPERSION

Parameters of the flow simulation

Coming from the previous results on the flow field simulation, we have choosen 64x64x64 grid cells, uniformely distributed in the three spatial direction The Reynolds number based on δ_0 is 400 and the convective Mach number is 0.8. Amplitudes of the disturbances are $A_1 = A_2 = 0.025$. Initially, 64x64x64 particles are seeded uniformely in the computational domain (one particle per cell) and particle velocity at the beginning of the calculation in each computational cell is the same of the fluid velocity in the cell. Dispersion of particles with Stokes numbers ranging from 0.1 to 1000 were simulated. Since there are periodic boundary conditions in the streamwise and spanwise directions, particles which move out of the box in these two directions from one side will be put back in the domain from the other side. Particles which move out the box in the cross-stream direction will not be recovered.

Resuls of particle dispersion

On figure 3 is summarized the evolution of the root mean square of particle number per cell over the whole field versus the Stokes number for different times. It is defined by

$$N_{rms} = \left(\sum_{i=1}^{N_c} N_i^2/N_c\right)^{1/2} \qquad (10)$$

Here $N_c = 64\text{x}64\text{x}64$ and at time $t = 0$,$N_{rms} = 1$. This quantity is used to determine the overall concentration character of particles.

It is obvious that particles with Stokes numbers close to unity have larger N_{rms} value which is similar to the results of Lin et al. (1998). It should be noted that unlike incompressible flows simulations, here three dimensional Λ large scales structures strongly affect the dispersion even in the early stages of the mixing layer destabilization. Indeed, we don't observe two dimensional pairing like in incompressible shear layer. This can be clearly seen on figure 2 where a perspective view of a pressure surface, that enclose a minimum of pressure (associated with strong rotation) is shown.

In order to examine the dispersion patterns for the different Stokes numbers, we have used the plane concept already defined in Lin et al. (1998). It corresponds to a thin slice with a thickness of a computational cell. Indeed, for the (x,z) plane at $y = L_y/2$, it means a thin slice with $L_y/2 < y < L_y/2 + \Delta y$, where Δy is the mesh spacing in the y direction.

We have drawn on the figure 4 the distribution of the particle in the plane (x,z) at $y = L_y/2$ at time $t = 26$. For the smallest Stokes number, the particles seem to follow quite closely the fluid particles, particles with Stokes number close to unity tend to accumulate around the edge of the three dimensional large scale structures. For larger Stokes numbers, the dispersion of particles in cross-stream direction is decreasing, indeed the particles are less influenced by the Λ shaped vortices. On the figures 5, are drawn the particle distribution in the plane $z = 0$. The accumulation of the particle with Stokes number of unity on the edge of the vortex is clearly seen on that figure. Thoses particles trace the projection of the three dimensional coherent structures on that plane. On the figure 6, the particle distribution in the plane $x = L_x/2$ is plotted. Here again, the structure projection on this plane is obvious when one looks at particle of $St = 1$ locations. Actually, theses particles seem to roll up around the arms of the λ vortex in an helicoidal way.

From this plane cut, particles with $St = 10$ show a quite different behaviour. Clearly, thoses particles are less sensitive to the vortex, there is no such accumulation at the egde of the vortex arms, even if void zone is present inside the vortex. For greater particle Stokes number, there is no more effect of the 3D vortex on the particle distribution, only a wavy movement can be seen on this plane cut.

In order to quantify the influence of those structures on particle dispersion the root mean square of particle number per cell for (y,z), (x,z), (x,y) planes, $N_{rms}(x)$, $N_{rms}(y)$, $N_{rms}(x)$ has been evaluated at time $t = 26$ (figures 7(a), 7(b), 7(c)) for various Stokes numbers. For example $N_{rms}(x)$ is defined by :

$$N_{rms}(x) = \left(\sum_{i=1}^{N_{cp}} N_i^2(x)/N_{cp}\right)^{1/2} \qquad (11)$$

where N_{cp} is the total number of computational cells in the plane (y,z) and $N_i(x)$ is the number of particles in the ith cell of that plane. The same definition is used for the two others quantities $N_{rms}(y)$ and $N_{rms}(z)$.

On the figure 7(a), we can observe how the particles with different Stokes numbers concentrate along the streamwise direction. The maximum concentration is obtained for

particle of unity Stokes number, when concentration is minimal for small and larger Stokes numbers. Moreover, the trend observed on that figure for the Stokes number which gives the maximum concentration, is completely opposite to that obtained for incompressible shear layer Lin et al. (1998). Even though for the incompressible case, $N_{rms}(x)$ is maximum at the boundaries of the computational box in x direction (for x near 0 and x near L_X) and minimal elsewhere, here $N_{rms}(x)$ is maximum in the center of the box (in x direction) and minimal at the boundaries. This emphasizes that dispersion mecanismes are really different in the two cases.

The next figure 7(b) gives the particles accumulation for the spanwise y direction. The same conclusions as in the previous figure can be drawn. The local minima observed for Stokes number of 1 show the trace of the arms of the λ vortex whereas Stokes number of 10 particle present in that zone a local maxmium.

The figure 7(c) shows the particle accumulation in the cross-stream direction. Due to the lack of pairing of spanwise vortex, the maximum concentration for the different Stokes number is restricted to a zone of size $2\delta_0$ centered at $z = 0$.. Maximum concentration is obtained for Stokes number 1 particles. This is consistant with the fact that supersonic shear layer gives rate of growing much smaller than incompressible one.

From that three figures, the level of concentration in the three direction is much lower compared to the incompressible case. This shows that particle dispersion is our case much more tridimensional than in the incompressible case.

To give one more insight in the way particles are dispersing in that kind of flow we have plot on the figures 8(a), 8(b), 8(c), 8(d) points representing the cells which contain at least three particles for the Stokes numbers 0.1, 1, 10, 100 respectively. Moreover superimposed on thoses figures is an isosurface corresponding to a pressure mimium which encloses the core of the Λ vortex. We have used a vertical clipping plane parallel to one of the arms of the vortex to cut the isosurface so that one can see inside the vortex core the presence of particles.

It is obvious on the figure 8(b), that Stokes number 1 particles are depleted from the vortex core and are twisted around the surface of the vortex in an helicoidal way and form a kind of filaments. The green and turquoise points on that figure correspond to cells where particle number is important whereas the purple points correspond to cells where particle number is 3.

For the smallest particle Stokes number, we can see that one can find particles inside the vortex, although the concentration seems to be more homogeneous than in the previous even if a zone located at the head of the Λ vortex contains green points.

Finally, for the two greatest particle Stokes numbers on figures 8(c) and 8(d), one can see vortex arms are filled by particles. Again, this is showing the weak influence of the vortex on the particle dispersion.

CONCLUSION

Direct numerical simulation of particles dispersion in supersonic 3D mixing-layer have been done. First comparisons with the incompressible case show important differences due to strong three-dimensionality of such flows. Particle with Stokes number close to unity are centrifugated at the periphery of large scale vortices. Because of the Λ shape of those vortices and because no pairing of two-dimensional structure is present, dispersion behaviour is very different from the incompressible case.

REFERENCES

Lin, W., Chung, J.N., Troutt, T.R., and Crowe, C.T., 1998 "Direct numerical simulation of a three-dimensionnal temporal mixing layer with particle dispersion", *Journal of Fluid Mechanics*,Vol 358, pp 61-85

Jacquin, L., Mistral , S., Geffroy, P., and Losfeld, G., 1991 "Etude d'un jet supersonique coaxial chauffé", *Rapport final ONERA*

Sandham, N.D., Reynolds, W.C., 1991, "Three-dimensionnal simulations of larges eddies in the compressible mixing layer", *Journal of Fluid Mechanics*,Vol 224, pp 133-158

Pierrhumbert, R.T., Widnall, S.E., 1982, "The two and three dimensional instabilities of a spatially perodic shear layer", *Journal of Fluid Mechanics*,Vol 144, pp 59-62

Chein, R., Chung, J.N., 1988, "Simulation of particle dispersion in a two-dimensionnal mixing layer", *AIChE Journal*,Vol 34, pp 946-954

Crowe, C.T., Chung, J.N., and Troutt, T.R., 1988, "Particle mixing in free shear layer ", *Prog. Energy Combust. Science*, Vol 14, pp 171-194

Tong, X.L., Wang, L.P., 1997, "Direct simulation of particle transport in a two and three-dimensionnal mixing layer", *Proceedings of the ASME Fluids Engineering Division Summer Meeting*

Gottlieb, D., Turkel, E., 1976, " Dissipative Two-Four Methods for Time Dependent Problems ", *Mathematics of Computation* , Vol 30, pp 703-723

Thompson, K.W., 1987, " Time Dependent Boundary Conditions for Hyperbolic Systems I ", *Journal of Computational Physics* , Vol 68, pp 1-24

Gamet, L., Estivalezes, J.L., 1995, " Non-reflexive Boundary Conditions applied to Jet Aeroacoustics. ", *AIAA Paper 95-0159*

Ragab, S.A. and Sheen, S.C., 1991, " Large-Eddy Simulation of a Mixing Layer", *AIAA Paper 91-0233*

Ragab, S.A. Sheen, S.S. and Sreedhar, M., 1992, "An Investigation of Finite-Difference Methods for Large-Eddy Simulation of a Mixing Layer", *AIAA Paper 92-0554*

Ducros, F., 1995, "Simulations numériques directes et des grandes échelles de couches limites compressibles.", *PhD Thesis, University of Grenoble*

Mankbadi, R.R., Hayder, M.E. and Povinelli, L.A., 1994, " The Structure of Supersonic Jet Flow and its Radiated Sound.", *AIAA Journal*,pp 897-906, 5, Vol 32

Bayliss, A., Parikh, P., Maestrello, L. and Turkel, E., 1985, " A Fourth-Order Scheme for the Unsteady Compressible Navier-Stokes Equations ", *AIAA Paper 85-1694*

Tang, W., Komerath, N. and Sankar, L., 1989, " Numerical Simulation of the Growth of Instabilities in Supersonic Free Shear Layers", *AIAA Paper 89-0376*

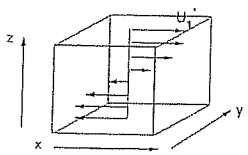

Figure 1. Temporal three dimensional mixing layer

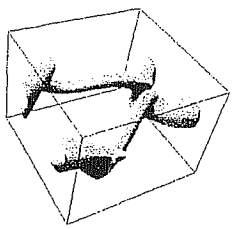

Figure 2. Isosurface of min pressure at time =20

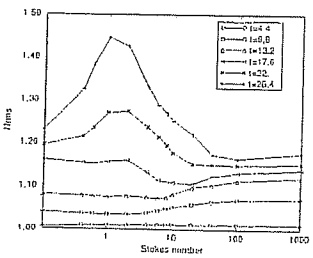

Figure 3. Root Mean Square of particle number per cell for different Stokes numbers

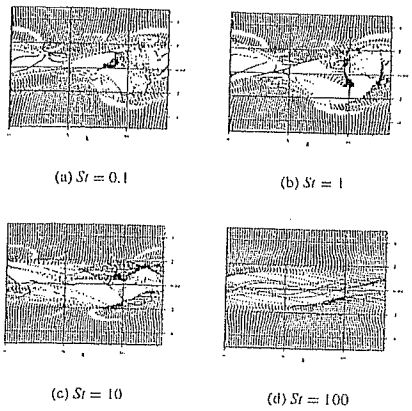

(a) $St = 0.1$ (b) $St = 1$

(c) $St = 10$ (d) $St = 100$

Figure 4. Plan cut at $y = L_y/2$ at $t = 26$

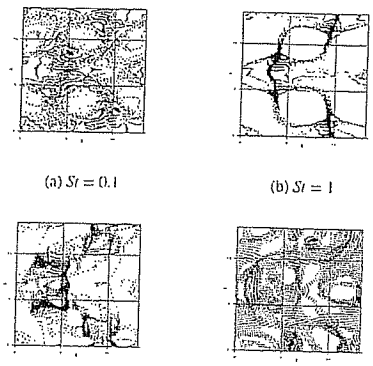

(a) $St = 0.1$ (b) $St = 1$

(c) $St = 10$ (d) $St = 100$

Figure 5. Plan cut at $z = 0$ at $t = 26$

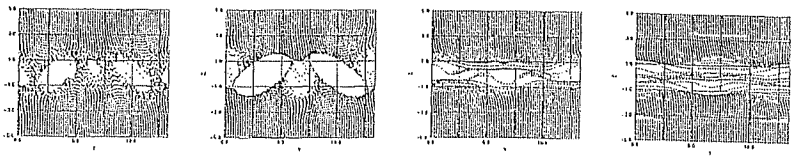

(a) $St = 0.1$ (b) $St = 1$ (c) $St = 10$ (d) $St = 100$

Figure 6. Plan cut at $x = L_x/2$ at $t = 26$

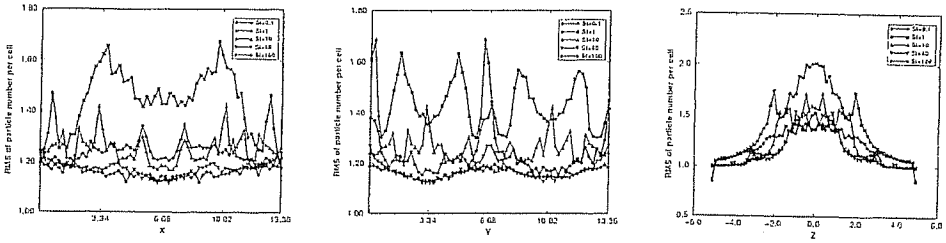

(a) $N_{rms}(x)$ at time t=26 (b) $N_{rms}(y)$ at time t=26 (c) $N_{rms}(z)$ at time t=26

Figure 7. N_{rms} by direction at time t=26

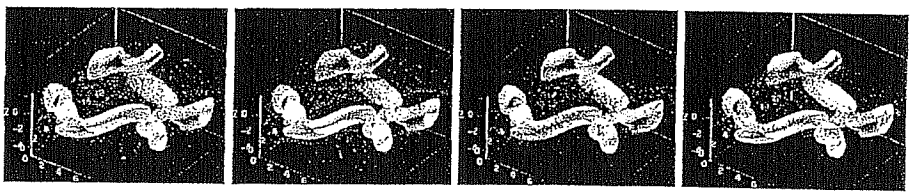

(a) Particles number ≥ 3, $St = 0.1$ (b) Particles number ≥ 3, $St = 1$ (c) Particles number ≥ 3, $St = 10$ (d) Particles number ≥ 3, $St = 100$

Figure 8. Particles visulisation